

Characterization of the Spectral Accuracy of an Orbitrap Mass Analyzer Using Isotope Ratio Mass Spectrometry

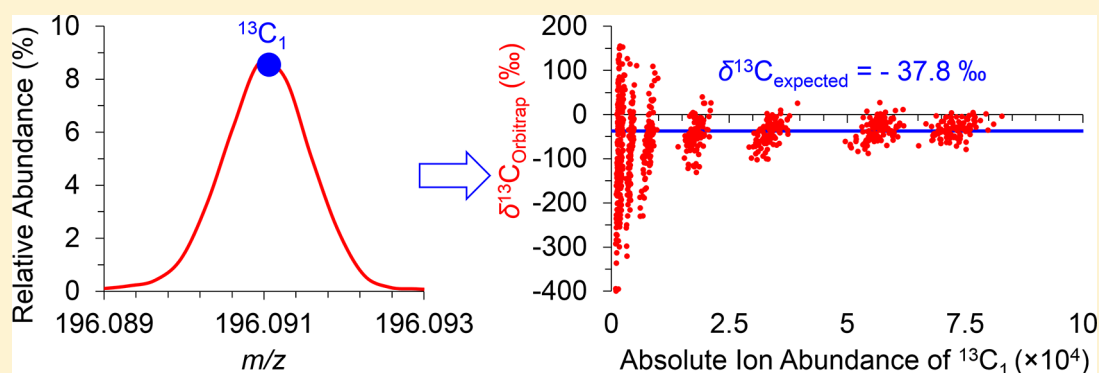
Sitora Khodjanizayova,^{†,‡} Milad Nazari,^{†,‡} Kenneth P. Garrard,^{†,‡} Mayara P. V. Matos,^{§,||} Glen P. Jackson,[§] and David C. Muddiman^{*,†}

[†]Department of Chemistry and Molecular Education, Technology, and Research Innovation Center (METRIC), North Carolina State University, Raleigh, North Carolina 27695, United States

[‡]Precision Engineering Consortium, Department of Mechanical and Aerospace Engineering, North Carolina State University, Raleigh, North Carolina 27606, United States

[§]Department of Forensic and Investigative Science and ^{||}Department of Biology, West Virginia University, Morgantown, West Virginia 26506, United States

S Supporting Information



ABSTRACT: Infrared matrix-assisted laser desorption electrospray ionization (IR-MALDESI) source coupled to the Q Exactive Plus has been extensively used in untargeted mass spectrometry imaging (MSI) analyses of biological tissue sections. Although the Orbitrap is a high-resolution and accurate-mass (HRAM) mass analyzer, these attributes alone cannot be used for the reliable identification of unknown analytes observed in complex biological matrices. Spectral accuracy (SA) is the ability of the mass spectrometer to accurately measure the isotopic distributions which, when used with high mass measurement accuracy (MMA), can facilitate the elucidation of a single elemental composition. To investigate the effects of different ion populations on an Orbitrap's SA and MMA, a solution of caffeine, the tetrapeptide MRFA, and ultramark was analyzed using a Q Exactive Plus across eight distinct automatic gain control (AGC) targets. The same compounds from the same lot numbers were also individually analyzed using isotope ratio mass spectrometry (IRMS) to accurately determine the isotopic abundance of ^{13}C , ^{15}N , and ^{34}S . We demonstrated that at optimum absolute ion abundances the Orbitrap can be used to accurately count carbons, nitrogens, and sulfurs in samples with varying masses. Additionally, absolute monoisotopic ion abundances required for high SA were empirically determined by using the expected (IRMS) and experimental (Orbitrap) isotopic distributions to calculate the Pearson chi-square test. These thresholds for absolute ion abundances can be used in untargeted MSI studies to shorten an identification list by rapidly screening for isotopic distributions whose absolute ion abundances are high enough to accurately estimate the number of atoms.

Accurate determination of elemental compositions is one of the most challenging aspects in untargeted metabolomics analyses.¹ High resolving power coupled with high mass measurement accuracy (MMA) alone cannot be used for confident identification of unknowns^{2–5} because, even at high MMA (<1 ppm), several elemental compositions are possible.^{5–7} However, high MMA combined with spectral accuracy (SA) can often lead to elucidation of a single elemental composition and/or confirmation of a database hit.^{6,8} In fact, using solely isotopic distributions can remove >95% of false candidates.⁶ Spectral accuracy is the ability of the mass

analyzer to accurately measure isotopic distributions (including isotopic fine structures) which, when coupled with high MMA, can be used for estimating the number of specific elements in an unknown.^{4,5,7–15} For example, to estimate the number of carbon atoms in a molecule, the relative abundance of A+1 ($^{13}\text{C}_1$) peak is divided by the natural abundance of ^{13}C on Earth ($\sim 1.11\%$) based on natural abundance values reported by the

Received: September 28, 2017

Accepted: December 27, 2017

Published: December 27, 2017

National Institute of Standards and Technology (NIST) or International Union of Pure and Applied Chemistry (IUPAC).¹⁶ However, the values in these libraries are presented as “best-measurement” values, whereas the true isotopic abundances fall somewhere within the observed range of natural variations.¹⁶ For instance, the relative abundance of ¹³C in terrestrial matter actually ranges from 0.96% to 1.15%, which provides sufficient variance to cause incorrect assessments of the number of carbons in a molecule.¹⁶

The motivation of the present work is to characterize SA of the Orbitrap mass analyzer^{2,17–19} based on the absolute ion abundances to allow its use in untargeted mass spectrometry imaging (MSI) studies with infrared matrix-assisted laser desorption electrospray ionization (IR-MALDESI)^{20,21} coupled to the Thermo Fisher Scientific Q Exactive Plus mass spectrometer.²² IR-MALDESI is an ambient ionization source where a mid-IR laser is used to desorb neutral species from a sample. The desorbed materials partition into the charged droplets of an orthogonal electrospray, where ions are formed in an ESI-like fashion.²⁰ These ions are next stored in the C-trap for a predetermined amount of time, denoted by the maximum injection time (IT),²³ and the automatic gain control (AGC) function in the Q Exactive Plus mass spectrometer is disabled due to the pulsed nature of the IR-MALDESI source. While MS/MS analyses can be performed on peaks of interest to confirm the structure of putative identifications,²² acquiring MS/MS spectra for every analyte in every voxel is virtually impossible in untargeted MSI analyses. Therefore, identification of unknowns in untargeted IR-MALDESI studies relies solely on MMA and SA. Nazari et al. have previously demonstrated the utility of SA and sulfur counting in the identification of metabolites in an untargeted polarity switching MSI analysis,⁷ where analyte was confidently identified from four potential candidates generated in MELTIN database.²⁴

One critically important and limiting factor in accurately characterizing the SA of a mass analyzer is the fact that there is a variation in the relative abundance of different isotopes of each element found in nature. Thus, to investigate the effects of absolute ion abundance on the Orbitrap's ability to recover expected isotopic distributions, we characterized known compounds spanning a wide mass range using isotope ratio mass spectrometry (IRMS) to accurately measure abundance of stable isotopes. Results from IRMS analyses allowed us to precisely monitor changes in relative abundances of ¹³C₁, ¹⁵N₁, and ³⁴S₁ molecular ions measured using the Q Exactive Plus. We report two experimentally determined optimal conditions for each of three arbitrarily defined mass windows of small (100 < MW (Da) < 400), medium (400 < MW (Da) < 900), and large (1000 < MW (Da) < 1500) compounds: (1) optimum absolute ¹³C₁, ¹⁵N₁, and ³⁴S₁ ion abundance for accurate carbon, nitrogen, and sulfur counting, respectively, and (2) thresholds for the absolute monoisotopic ion abundances required for high SA. In the work presented here, we demonstrate that it is crucial to establish thresholds for absolute ion abundances because changes in the absolute ion abundance could influence the MMA and SA and subsequently hinder the ability to confidently identify unknown analytes. Establishing the optimum absolute ion abundances required for high MMA and SA will help to reduce the number of potential identifications (IDs), generated by searching the accurate mass in databases such as METLIN²⁴ or HMDB,²⁵ because compounds whose absolute ion abundances are above certain thresholds can be used for confident estimation of elemental

compositions. Once a narrow list of potential IDs is generated, a different algorithm can be used to predict the elemental compositions of those compounds that pass the first screening.^{4,7}

EXPERIMENTAL SECTION

Materials. Caffeine was purchased from both Sigma-Aldrich (St. Louis, MO) and the International Atomic Energy Agency (IAEA). The two caffeine samples are termed caffeine_{Sigma} and caffeine_{IAEA}, respectively. The tetrapeptide MRFA acetate salt and acetic acid were also purchased from Sigma-Aldrich. HPLC-grade methanol, water, and acetonitrile were purchased from Burdick & Jackson (Muskegon, MI). Ultramark was purchased from ABCR GmbH (Karlsruhe, Germany).

The isotope standards of glutamic acid (USGS-40 and USGS-41) were obtained from the United States Geological Survey (USGS, Reston, VA). An isotope standard of sulfanilamide was purchased from IVA Analysentechnik e. K. (Meerbusch, Germany).

Direct Infusion of Caffeine, MRFA, and Ultramark Mixture Using Q Exactive Plus. In Q Exactive Plus analyses, a mixture of caffeine_{Sigma}, MRFA, and ultramark was ionized in the ESI interface. Neutral species were filtered in the bent flatapole whereas ions were efficiently transferred to the RF-only quadrupole mass filter. Exiting the quadrupole, ions were cooled in the C-trap²⁶ and injected into the Orbitrap for further image current detection and fast Fourier (FT) transformation.²⁷

The Q Exactive Plus mass spectrometer was calibrated prior to analyses. Caffeine_{Sigma}, MRFA, and ultramark were dissolved in 5 mL of acetonitrile, 4.68 mL of 50:50 methanol:water (v/v), and 100 μ L of acetic acid to yield a mixture containing 2 μ g/mL caffeine, 0.7 μ g/mL MRFA, and 18 μ g/mL ultramark. The mixture was directly infused into the Q Exactive Plus mass spectrometer using ESI at a flow rate of 2 μ L/min with the electrospray voltage and inlet temperature at 4.0 kV and 320 °C, respectively. The mixture was analyzed from m/z 150 to m/z 2000 with a resolving power of 140 000_{FWHM} at m/z 200. Ninety-nine transient scans (1 microscan each) were recorded at each of eight AGC targets: 2×10^4 , 5×10^4 , 1×10^5 , 2×10^5 , 5×10^5 , 1×10^6 , 3×10^6 , and 5×10^6 . The maximum IT for each injection was set to 100 ms to provide enough time for ion accumulation at high AGC targets. To achieve low ppm MMA, peaks of diisooctyl phthalate at m/z 391.2843 [M + H]⁺ and 413.2662 [M + Na]⁺ were used as lock-masses for internal calibration.²⁸

Direct Infusion of IRMS Reference Standards Using Q Exactive Plus. Each isotope reference standard was diluted in 5 mL of acetonitrile, 5 mL of 50:50 methanol:water (v/v), and 100 μ L of acetic acid to have four standards for direct infusion analysis: 0.03 mg/mL glutamic acid 1 (USGS-40), 0.002 mg/mL caffeine_{IAEA} (IAEA-600), 0.002 mg/mL sulfanilamide, and 0.03 mg/mL glutamic acid 2 (USGS-41). Glutamic acid 1, caffeine_{IAEA}, sulfanilamide, and glutamic acid 2 were directly infused one at a time into the Q Exactive Plus mass spectrometer in the listed order. A relatively narrow m/z range of 70–280 was measured to make sure that the mass of each reference standard fell roughly in the middle of selected m/z range.⁴ The AGC target and maximum IT were set to 1×10^6 and 300 ms, respectively, and 100 transient scans (1 microscan each) were obtained per analyte at a resolving power of 140 000_{FWHM} at m/z 200.

Even though analysis of narrow m/z ranges²⁹ with increased number of microscans³⁰ at higher RPs can improve SA, we used instrumental parameters that are more typical in untargeted MSI experiments (*e. g.*, wide m/z range, 1 microscan, RP = 140 000_{fwhm} at m/z 200) to demonstrate the applicability of this approach to more realistic untargeted IR-MALDESI MSI studies.

Analysis of Caffeine_{Sigma}, MRFA, and Ultramark Using IRMS. For the bulk isotope analysis of $\delta^{13}\text{C}$ and $\delta^{15}\text{N}$, samples of approximately 0.5 mg of caffeine_{Sigma}, 0.3 mg of MRFA, and 0.9 mg of ultramark were weighed in tin capsules and placed in a Thermo Flash HT Plus elemental analyzer (EA) coupled via a ConFlo IV interface (Thermo Finnigan, Waltham, MA) to a Thermo Delta V Advantage isotope ratio mass spectrometer. The elemental analyzer converted each sample (caffeine_{Sigma}, MRFA, or ultramark) into simple fixed gases (*e.g.*, N_2 , CO_2) using the standard combustion and a reduction reactor, followed by separation in a packed gas chromatography (GC) column using helium (Matheson, Fairmont, WV) as the carrier gas. The purified gas molecules were subsequently ionized via electron ionization (EI), and the abundances of these ionized gases were detected simultaneously using multiple Faraday cups after passing through the magnetic sector mass analyzer.³¹ Data acquisition was carried out using Isodat 3.0 software (Thermo Finnigan, Waltham, MA).

Carbon isotope ratios were measured relative to a compressed reference CO_2 gas (Airgas, Morgantown, WV) and normalized to the international scale relative to Vienna Pee Dee Belemnite (VPDB) using a two-point linear regression calibration based upon the certified reference materials USGS-40 (-26.39‰) and USGS-41 ($+37.63\text{‰}$).³² The correction for ^{17}O was performed using the standard Santrock algorithm.³³ For nitrogen isotope ratios, delta values were measured relative to compressed nitrogen (Airgas, Morgantown, WV) and were normalized to international air N_2 using a two-point calibration curve composed of USGS-40 (-4.52‰) and USGS 41 ($+47.57\text{‰}$). Triplicate measurements of each sample provided mean values and 95% confidence intervals, which were reported on the per mill (‰) scale relative to VPDB for $\delta^{13}\text{C}$ and air for $\delta^{15}\text{N}$.

Sulfur bulk isotope ratios of MRFA samples were measured by the United States Geological Survey (Reston Stable Isotope Laboratory, Reston, VA) using a continuous flow isotope ratio mass spectrometer.³⁴ Results were reported in per mill (‰) relative to Vienna-Canyon Diablo Troilite (VCDT) and defined by assigning an exact value of -0.3‰ to IAEA-S-1 (silver sulfide),³⁵ and no correction was conducted for oxygen isotopic composition.

Data Analysis. To correctly assign peaks in isotopic distributions measured using the Q Exactive Plus, theoretical exact molecular masses were calculated using exact atomic mass values reported by IUPAC.¹⁶ To avoid confusion, we refer to ultramark as ultramark 1421 throughout this manuscript because in data analysis we focused only on the most abundant $[\text{M} + \text{H}]^+$ ion at m/z 1421 (Figure S-1). The .RAW files generated by the Q Exactive Plus were processed in XCalibur software (version 2.2, Thermo Fisher Scientific, San Jose, CA) and then converted into the .mzML format using the open-source MSConvertGUI tool from ProteoWizard.²⁹ Subsequently, the m/z values within ± 2.5 ppm tolerance were extracted using the RawMeat tool (version 2.1, VAST Scientific, Cambridge, MA) and exported into Excel. Masses for isotopologues were calculated using the difference in their

exact masses from the monoisotopic peak. Extracted ion chromatograms (XIC) for each peak (± 2.5 ppm) were generated using XCalibur and exported into Excel. We exported IT for each transient scan to calculate the absolute ion abundances (abundance from .RAW file [in ions/seconds] \times IT [in seconds]) because prescanned AGC targets result in slightly different ITs from scan to scan. All subsequent analyses and calculations were performed in Excel.

RESULTS AND DISCUSSION

Orbitrap's Sensitivity of Measuring Relative Abundances across Eight AGC Targets. We characterized the Orbitrap's performance in a Q Exactive Plus mass spectrometer at a resolving power of 140 000_{fwhm} at m/z 200 by altering AGC targets to monitor how different ion populations affect mass and spectral accuracy in arbitrarily defined small ($100 < \text{MW} (\text{Da}) < 400$), medium ($400 < \text{MW} (\text{Da}) < 900$), and large ($1000 < \text{MW} (\text{Da}) < 1500$) compounds represented by caffeine_{Sigma} ($\text{C}_8\text{H}_{10}\text{N}_4\text{O}_2$), MRFA ($\text{C}_{23}\text{H}_{37}\text{N}_7\text{O}_5\text{S}$), and ultramark ($\text{C}_{28}\text{H}_{18}\text{O}_6\text{N}_3\text{P}_3\text{F}_{24}(\text{C}_2\text{F}_4)_n$, $n = 0-12$). The effects of varying the resolving power were not investigated in this study because this topic has already been discussed in detail by others.^{4,9,10} We prepared a homemade positive ion calibration solution from caffeine, MRFA, and ultramark to have materials from the same lot numbers for IRMS analyses. The homemade calibration solution had smaller concentrations of caffeine_{Sigma} ($2\text{ }\mu\text{g/mL}$) and MRFA ($0.7\text{ }\mu\text{g/mL}$) relative to commercial Thermo Scientific Pierce LTQ ESI Positive Ion Calibration Solution, which usually has caffeine and MRFA concentrations of $20\text{ }\mu\text{g/mL}$ and $1\text{ }\mu\text{g/mL}$, respectively. The full range spectrum in Figure S-1 shows that the relative abundances in homemade calibration solution differ quite substantially from the relative abundances normally seen in the spectrum of the commercially available calibration solution.

As mentioned above, SA in tandem with high MMA can be used for confident elucidation of unknown analytes. As expected, in lock-mass controlled analyses, MMAs for caffeine_{Sigma}, MRFA, and ultramark fell within the accepted range of ± 2.5 ppm across all eight AGC targets. Moreover, with larger ion populations, MMA for caffeine_{Sigma}, MRFA, and ultramark approached ~ 0.6 ppm, ~ 0.7 ppm, and ~ 0.6 ppm, respectively (Figure S-2). However, MMA alone cannot be used for accurate identification of unknown compounds with complex elemental compositions.⁶ Once it was shown that the MMA was preserved at all ion populations, we turned our attention to characterizing how accurately the Orbitrap measures relative abundances of stable isotopologues such as $^{13}\text{C}_1$, $^{15}\text{N}_1$, and $^{34}\text{S}_1$ that can be used in carbon, nitrogen, and sulfur counting, respectively.

To ensure the most accurate characterization of the Orbitrap's SA, the relative abundances of the stable isotopes in caffeine_{Sigma}, MRFA, and ultramark were measured using EA-IRMS. The values were reported using the δ notation in units of parts per thousand, or per mill (‰). δ stands for the difference in isotopic composition of the analyte relative to that of the reference standard.³¹ The same compounds (caffeine_{Sigma}, MRFA, and ultramark) from the same lot numbers were mixed together and directly infused into the Q Exactive Plus mass spectrometer by ESI and analyzed at the eight different AGC targets. Knowing the elemental composition of each of the three compounds, we were able to convert abundances measured with Q Exactive Plus into atom percent (isotope's natural abundance) and calculate the δ values to monitor how

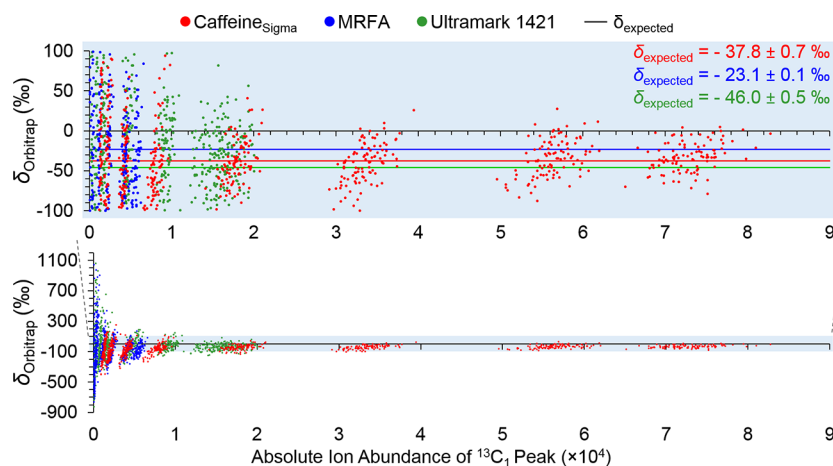


Figure 1. Dependence of calculated $\delta_{\text{Orbitrap}}^{13\text{C}}$ on absolute ion abundance of A+1 ($^{13}\text{C}_1$) peak using caffeine_{Sigma}, MRFA, and ultramark 1421. $\delta_{\text{expected}}^{13\text{C}}$ values with 95% confidence interval, as measured by IRMS, are shown on the top right and are also depicted as solid lines on the figure. The inset on top shows the zoomed-in region of -100 to 100 on the y-axis. Each data point represents a single transient scan.

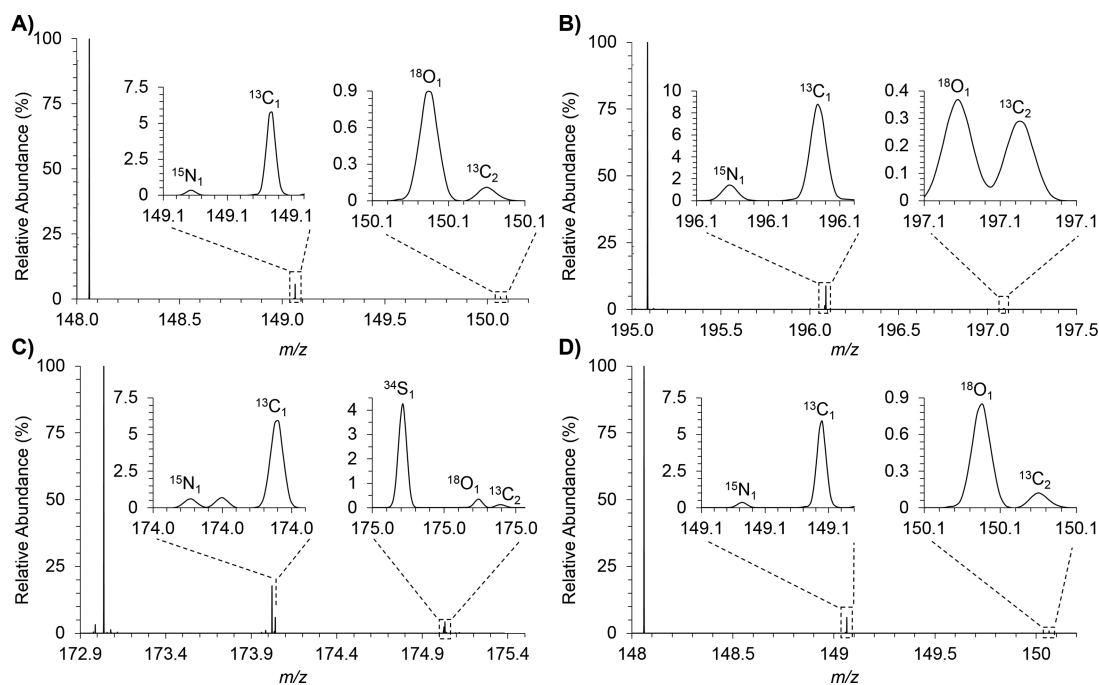


Figure 2. Orbitrap mass spectra collected in positive ESI mode at RP_{fwhm} of 140 000 at m/z 200 for (A) glutamic acid 1 (USGS-40), (B) caffeine_{IAEA} (IAEA-600), (C) sulfanilamide, and (D) glutamic acid 2 (USGS-41) that were injected separately one sample at a time. User-defined AGC target for each injection was set to 1×10^6 and acquired m/z range was 70–280. Instrument-determined average injection time ($n = 100$ transient scans) for glutamic acid 1, caffeine_{IAEA}, sulfanilamide, and glutamic acid 2 was 4, 21, 14, and 4 ms, respectively.

spectral accuracy changed across eight AGC targets. First, the abundances (from .RAW files) measured using the Orbitrap were used to calculate the abundance ratios of the heavier isotope (e.g., ^{13}C) to the lighter isotope (e.g., ^{12}C) of each atom in a given analyte. The ratios were then normalized to the number of atoms as shown in eq 1:

$$R_{\text{sample}} = \frac{\text{abundance of A+1}}{(\text{abundance of A}) \times \text{no. of atoms}} \quad (1)$$

R_{sample} ratios were then used to calculate the atom percent (atom %) and δ values for each atom according to eqs 2 and 3, respectively:

$$\text{atom\%} = \frac{R_{\text{sample}}}{1 + R_{\text{sample}}} \times 100 (\%) \quad (2)$$

$$\delta = \left(\frac{R_{\text{sample}}}{R_{\text{standard}}} - 1 \right) \times 1000 (\text{‰}) \quad (3)$$

R_{standard} in eq 3 represents the same ratio as R_{sample} but for a standard reference material that is naturally enriched in stable isotopes. Ion abundances measured in the Orbitrap were converted into δ_{Orbitrap} and plotted against absolute ion abundances of $^{13}\text{C}_1$ isotopologues for all three compounds as shown in Figure 1. The mean δ_{expected} values and their corresponding 95% confidence intervals, measured using IRMS, are shown on the top right of the Figure 1. Mean

δ_{expected} values are also depicted as solid lines on the graph for easier visualization. It can be seen that the calculated $\delta_{\text{Orbitrap}}^{13\text{C}}$ for caffeine_{Sigma}, MRFA, and ultramark 1421 approach $\delta_{\text{expected}}^{13\text{C}}$ as the absolute ion abundances increase; however, even with large ion populations, $\delta_{\text{Orbitrap}}^{13\text{C}}$ does not fall within the 95% confidence interval of $\delta_{\text{expected}}^{13\text{C}}$. The values for $\delta_{\text{Orbitrap}}^{15\text{N}}$ and $\delta_{\text{Orbitrap}}^{34\text{S}}$ distributions in caffeine_{Sigma} and MRFA follow the same trend (Figure S-3).

To further investigate the ability of the Orbitrap to accurately measure isotope ratios at higher ion populations, four IRMS reference standards were directly infused into the Q Exactive Plus mass spectrometer individually and analyzed from m/z 70 to m/z 280 to have all four peaks fall roughly in the middle of the selected mass range (Figure 2). The key step in this analysis was injection of each reference standard one at a time with the prescanned AGC target and fixed maximum IT set to 1×10^6 ions and 300 ms, respectively. One hundred consecutive spectra were recorded to establish the mean and 95% CI for the reported isotope ratios. As shown in Table 1, $\delta_{\text{expected}}^{13\text{C}}$ and

Table 1. Analysis of Four IRMS Reference Standards Using a Q Exactive Plus^a

IRMS standards	isotopes	δ_{Orbitrap}	δ_{expected}
caffeine (IAEA-600)	¹⁵ N	-38 ± 48 (SD)	$+1.0 \pm 0.2$ (SD)
	¹³ C	-30 ± 19 (SD)	-27.77 ± 0.04 (SD)
glutamic acid 1 (USGS-40)	¹⁵ N	-80 ± 76 (SD)	-4.52 ± 0.06 (SD)
	¹³ C	-7 ± 21 (SD)	-26.39 ± 0.04 (SD)
glutamic acid 2 (USGS-41)	¹⁵ N	-19 ± 81 (SD)	$+47.6 \pm 0.1$ (SD)
	¹³ C	$+51 \pm 20$ (SD)	$+37.63 \pm 0.05$ (SD)
sulfanilamide	¹⁵ N	-130 ± 24 (95% CI)	-0.4 ± 0.2 (95% CI)
	¹³ C	-79 ± 10 (95% CI)	-27.8 ± 0.3 (95% CI)
	³⁴ S	-51 ± 14 (95% CI)	$+19.0 \pm 0.7$ (95% CI)

^aAbundances of ions of interest (¹⁵N₁, ¹³C₁, and ³⁴S₁) collected using the Q Exactive Plus were converted to δ notation (δ_{Orbitrap}) and compared to the expected values (δ_{expected}) measured using IRMS.

$\delta_{\text{expected}}^{15\text{N}}$ in caffeine_{IAEA}, glutamic acid 1, and glutamic acid 2 are the only expected values to fall within the confidence interval of the measured isotope ratios ($\delta_{\text{Orbitrap}}^{13\text{C}}$ and $\delta_{\text{Orbitrap}}^{15\text{N}}$). The rest of the δ_{expected} values do not fall within the confidence interval of the calculated δ_{Orbitrap} values. As we predicted, all the $\delta_{\text{Orbitrap}}^{13\text{C}}$ values measured with the Orbitrap have much lower precision in comparison to $\delta_{\text{expected}}^{13\text{C}}$ measured using IRMS. These results suggest that even at seemingly optimized parameters that result in ideal MMA, the Q Exactive Plus cannot measure ¹³C/¹²C, ¹⁵N/¹⁴N, and ³⁴S/³²S isotope ratios as accurately and precisely as IRMS.

The typical precision (95% CI) of IRMS measurements is on the order of 0.2‰ for carbon and 0.3‰ for nitrogen, whereas the Orbitrap provided pooled confidence intervals on the order of 9‰ for carbon and 17‰ for nitrogen. The Orbitrap is therefore approximately 50 times less precise than the IRMS. Heisenberg's uncertainty principle implies that the amplitude and the frequency of an image current in the Orbitrap cannot simultaneously be known to high degrees of confidence, and that the better one knows the time domain (i.e., the frequency,

and therefore the m/z), the worse one knows the amplitude, or ion abundance.³⁶ Miladinovic et al. have shown that FT-ICRs are capable of precisions on the order of 1 ppm in the time domain but at the expense of only ~1% precision in the abundance domain.³⁷ The main advantage of multicollector magnetic sector instruments comes from the ability to measure isotope abundances simultaneously on at least two detectors and for extended durations. These two features compensate for ion source variation over time and enable more signal averaging, which both lead to better precision. After obtaining such high precision, one must only then correct for any bias in the instrument and detection system, which is readily accomplished through comparison of unknowns to isotope standards. Also, in IRMS analyses, each sample is converted into simple pure gases before analysis and thus abundances of isotopes are measured on the atomic level. In contrast, the Orbitrap measures relative abundances of molecular ions with different isotopic compositions.^{18,38,39} Therefore, in FT-based measurements, such as the Orbitrap, it is oftentimes not possible to independently measure abundances of all the contributing isotopic ions, so approximations and assumptions must be made regarding the abundance of unresolved isotopes. For instance, the approximated expected relative abundance of A+1 (¹³C₁) will always be slightly larger than the true relative abundance of A+1 (¹³C₁) peak because expected relative abundance of A+1 is the product of the number of atoms and the atom percent of ¹³C from all isotopologues.

Orbitrap's Sensitivity of Carbon Counting across Eight AGC Targets. To calculate the expected relative abundance of ¹⁵N₁, ¹³C₁, and ³⁴S₁ peaks, accurate atom percent values obtained from IRMS were multiplied by the total number of atoms of interest in a molecule. Because IRMS measures the abundance ratio of one heavy (e.g., ¹³C) to one light isotope (e.g., ¹²C), we used eq 4 for computing the binomial probability distribution to estimate the abundance of the A+2 peak in a molecule with a total of N atoms of interest (e.g., ¹³C₂ peak):

$$P(n) = \frac{N!}{n!(N-n)!} p^n (1-p)^{N-n} \quad (4)$$

In eq 4, n is the isotopic peak ($n = 0$ being monoisotopic peak A and $n = 1$ is the A+1 peak, etc.), N is the total number of atoms of interest, and $0 < p < 1$ is the relative abundance (RA) of the stable isotope. The expected relative abundance of each $n > 1$ peak was calculated using eq 5:

$$\text{expected RA} = \frac{P(n)}{P(0)} \times 100\% \quad (5)$$

Figure 3 shows representative mass spectra for ultramark 1421, caffeine_{Sigma}, and MRFA collected with Q Exactive Plus at a resolving power of 140 000_{fwhm} at m/z 200 and AGC targets of 2×10^5 , 5×10^5 , and 3×10^6 , respectively. At these AGC targets all three compounds have relative abundances that best match their expected relative abundances depicted as red dots and calculated using δ values from IRMS analyses. Note that in Figure 3A there is no red dot above ¹⁸O₁ peak because we measured only carbon and nitrogen isotope ratios in caffeine_{Sigma}. It can be seen that ¹³C₁ and ¹⁵N₁ peaks are only baseline resolved in caffeine_{Sigma}, whereas in heavier molecules such as ultramark 1421, the ¹⁵N₁ peak is not resolved from the ¹³C₁ peak. In addition to the A+1 peaks, the A+2 peaks of caffeine_{Sigma} (¹⁸O₁ and ¹³C₂) and MRFA (³⁴S₁ and ¹³C₂) are

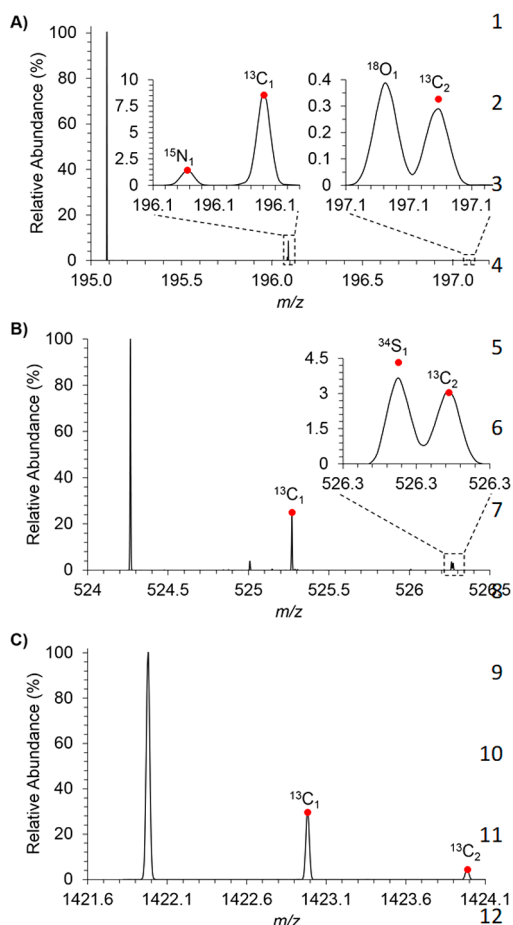


Figure 3. Representative Orbitrap mass spectra for (A) caffeine_{Sigma}, (B) MRFA, and (C) ultramark 1421 collected in positive ESI mode at RP_{fwhm} of 140 000 at m/z 200 and AGC targets of 5×10^5 , 3×10^6 , and 2×10^5 , respectively. Each spectrum was acquired within m/z range of 150–2000. Instrument-determined average injection times ($n = 99$ transient scans) for caffeine_{IAEA}, MRFA, and ultramark 1421 was 1, 6, and 0.3 ms, respectively.

also resolved from each other. Figure 3 suggests that in general the Orbitrap slightly underestimates relative abundances of heavier isotopic species in isotopic distributions, specifically $\sim 12\%$ underestimation for $^{13}\text{C}_2$ in caffeine and $\sim 15\%$ for $^{34}\text{S}_1$

$$\text{known} - \text{observed no. of carbons} = \frac{(\text{known no. of carbons}) \times (^{13}\text{C} \text{ atom } \%) - (\text{observed RA of } ^{13}\text{C}_1)}{^{13}\text{C} \text{ atom } \%} \quad (6)$$

Atom percent values in eq 6 were determined using EA-IRMS and observed relative abundances (RA) were measured on the Q Exactive Plus. Using eq 6 with atom percent values from IRMS, we monitored how SA and thus Orbitrap's ability to count carbons (Figure 4), nitrogens (Figure S-5A), and sulfurs (Figure S-5B) was affected across eight AGC targets. Note that at smaller AGC targets, nitrogen in caffeine_{Sigma} (Figure S-5A) and sulfur in MRFA (Figure S-5B) were not resolved, and that is why there are seven and six data points in caffeine_{Sigma} and MRFA plots, respectively. Figures 4, S-5A, and S-5B demonstrate that the difference between known and expected number of atoms follows the same trend in each of the three compounds: the smallest difference is achieved roughly in the middle of the absolute ion abundance curve, and the larger

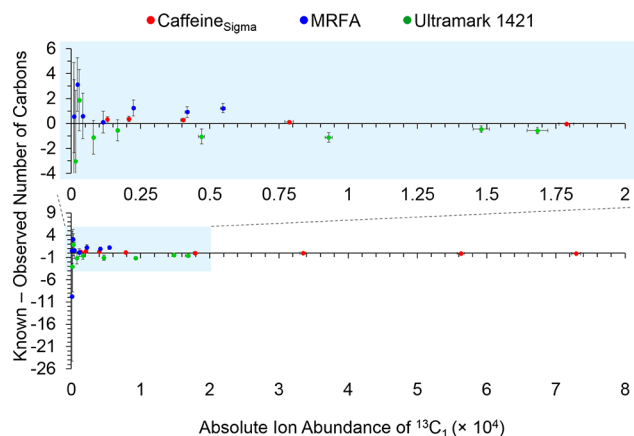


Figure 4. Deviations from the known number of carbons across different ion populations in caffeine_{Sigma}, MRFA, and ultramark 1421. Atom percent values, used in carbon counting, were obtained from IRMS analyses. Error bars correspond to 95% confidence interval of the mean ($n = 99$).

in MRFA. According to Su et al., this underestimation could be a result of interference between isotopic species of similar masses that oscillate at almost identical frequencies in the Orbitrap.⁹

To estimate the number of carbons in an unknown molecule, the relative abundance of $A+1$ ($^{13}\text{C}_1$) peak is divided by the natural abundance of ^{13}C . Most often the “best measurement” value from a database such as IUPAC is used for this process.⁸ However, using abundances from such databases for carbon counting does not result in accurate estimation of elemental compositions because not all compounds have the same relative ^{13}C abundance. For instance, the best measurement for ^{13}C atom percent from IUPAC is 1.108%, while in our analysis the atom percent values measured using IRMS are 1.070%, 1.086%, and 1.061% for caffeine_{Sigma}, MRFA, and ultramark 1421, respectively (Figure S-4). We used EA-IRMS atom percent values to measure how well the Q Exactive Plus is capable of counting carbons, nitrogens, and sulfurs when the atom percent is “known”. Using eq 6, we calculated the difference between known and observed number of carbons across different ion populations as shown in Figure 4:

difference is observed at the lowest and highest absolute ion abundances. It is worth noting that while the mean difference gets worse at high absolute ion abundances for MRFA (Figure 4), the precision of the measurement is still improved significantly. Moreover, Figure S-6 shows how the difference between expected and observed relative abundance of $^{13}\text{C}_2$ peak in MRFA improves at higher AGC targets. Note that at the smallest AGC target of 2×10^4 , the $^{13}\text{C}_2$ peak was indistinguishable from the signal-to-noise, and at AGC target of 5×10^4 , most of the $^{13}\text{C}_2$ peaks had signal intensity of zero. IRMS does not measure relative abundance of $^{13}\text{C}_2$ isotopologues, so in the probability equation we were estimating abundance of $^{13}\text{C}_2$ in MRFA based on an already known atom percent of ^{13}C from IRMS analysis. Relative

abundance of $^{13}\text{C}_2$ peak cannot be used in carbon counting, and this explains why we were mainly focusing on A+1 species.

“The highest ion population” in this study refers to the absolute ion abundance at the maximum AGC target (5×10^6), but more ions can be stored in the Orbitrap by disabling AGC target and setting maximum IT to a high number (e.g., 100 ms). However, when too many ions are injected into the Orbitrap (e.g., $\text{IT} \geq 100$ ms), molecular ions start experiencing space-charge effects, which result in suppressed abundance signals in lighter molecules and enhanced abundance signals in heavier molecules. Spectral accuracy is the most affected in the least abundant species because species with smaller ion cloud densities have much faster decay rates.⁴⁰ When comparing MS spectra of caffeine_{Sigma}, MRFA, and ultramark 1421 collected at prescanned AGC targets of 5×10^5 , 3×10^6 , and 2×10^5 , respectively, with spectra collected at IT of 100 ms with fixed AGC function, the absolute ion abundances of monoisotopic peaks shown in Table 2 changed significantly. At AGC targets

Table 2. Comparison of Absolute Monoisotopic Ion Abundances Acquired at Small (column 2) and Large (column 3) Total Ion Populations^a

	absolute ion abundance of A peak at optimum AGC targets	absolute ion abundance of A peak at IT = 100 ms
caffeine _{Sigma}	2.1×10^5 ions (AGC = 5×10^5)	2.3×10^3 ions
MRFA	1.8×10^4 ions (AGC = 3×10^6)	3.0×10^4 ions
ultramark 1421	5.6×10^3 ions (AGC = 2×10^5)	2.6×10^5 ions

^aNote that at “optimum AGC targets”, shown in column 2, experimental relative abundances (Orbitrap) match the expected relative abundances (IRMS) the best.

of 5×10^5 , 3×10^6 , and 2×10^5 , caffeine_{Sigma}, MRFA, and ultramark 1421, respectively, have relative abundances that best match the expected relative abundances measured using IRMS. Also, each of these AGC targets has maximum IT that is much shorter than 100 ms. Table 2 shows that at longer ITs, the absolute monoisotopic ion abundance decreased by 2 orders of magnitude in caffeine_{Sigma}, did not change much in MRFA, and increased by 2 orders of magnitude in ultramark 1421. As a result, relative abundance of A+1 ($^{13}\text{C}_1$) peak in caffeine was reduced by a factor of ~ 2 from 8.58% to 4.85%, while the expected relative abundance was 8.56% according to IRMS measurements. This was not the case for heavier molecules such as MRFA and ultramark 1421, which did not have significant changes in spectral accuracy at IT of 100 ms: the relative abundance of A+2 ($^{34}\text{S}_1$) peak in MRFA had an insignificant change from 3.76% (IT = 6.09 ms) to 3.75% (IT = 100 ms) while the expected relative abundance was 4.33%. Similarly, in ultramark 1421, observed relative abundance of $^{13}\text{C}_1$ peak changed slightly from 30.28% (IT = 0.33 ms) to 29.81% (IT = 100 ms) while expected relative abundance was 29.70%.

Figures 4, S-5A, and S-5B confirm that indeed there is an optimum number of injected ions that results in sufficient spectral accuracy to allow for accurate estimation of the number of carbons, nitrogens, and sulfurs. To accurately estimate the number of carbons with the desired precision of less than ± 0.5 atoms, the absolute $^{13}\text{C}_1$ ion abundance should be ~ 7.9 (± 0.15) $\times 10^3$ in caffeine_{Sigma} (± 0.12 atoms), ~ 1.1 (± 0.04) $\times 10^3$ in MRFA (± 0.11 atoms), and ~ 1.5 (± 0.03) $\times 10^4$ in ultramark 1421 (± 0.45 atoms) (Figure 4). It is worth noting

that optimum absolute ion abundance of MRFA peptide with charge state of +1 is 1 order of magnitude smaller than in ultramark 1421 and almost identical to abundance threshold in caffeine_{Sigma}. This is explained by MRFA's ionization efficiency at +1 charge state. Molecular ions of MRFA with charge state of +2 are much more abundant than ultramark 1421 and less abundant than caffeine_{Sigma}. Reliable nitrogen counting (± 0.31 nitrogens) in caffeine_{Sigma} is possible at absolute $^{15}\text{N}_1$ ion abundance of ~ 3.4 (± 0.22) $\times 10^2$ (Figure S5-A), and reliable sulfur counting (± 0.13 sulfurs) in MRFA can be achieved when absolute $^{34}\text{S}_1$ ion abundance is ~ 6.6 (± 0.31) $\times 10^2$ (Figure S5-B). Interestingly, when counting atoms with atom percent values from IUPAC at above-mentioned thresholds, we can still accurately estimate number of carbons (± 0.39 atoms, Figure S-7) and nitrogens (± 0.35 atoms, Figure S5-A) in caffeine_{Sigma} and sulfurs in MRFA (± 0.10 atoms, Figure S5-B). However, as expected, when counting carbons in MRFA and ultramark 1421 using atom percent values from IUPAC, the tolerance lowers to ± 0.56 and ± 0.76 atoms in MRFA and ultramark 1421, respectively. It is worth noting that, because the relative abundance of ^{34}S in nature is much higher than that of ^{13}C and ^{15}N , the tolerance window for sulfur counting can be wider compared to the tolerances used for carbon and nitrogen counting.

To estimate the minimum absolute monoisotopic ion abundance required for high spectral accuracy, we generated the Pearson chi-square (χ^2) distributions across eight AGC targets for each of the three test compounds (Figure 5). To calculate χ^2 values for relative abundances we used eq 7:

$$\chi^2 = \sum \frac{(\text{observed RA} - \text{expected RA})^2}{\text{expected RA}} \quad (7)$$

χ^2 for each compound was calculated by summing the χ^2 of an individual atom in the compound, depending on peak resolution:

$$\begin{aligned} \chi_{\text{caffeine}(\text{Sigma})}^2 &= \chi_{\text{C}}^2 + \chi_{\text{N}}^2 + \chi_{\text{O}}^2 \\ \chi_{\text{MRFA}}^2 &= \chi_{\text{C}}^2 + \chi_{\text{S}}^2 \\ \chi_{\text{ultramark}_{1421}}^2 &= \chi_{\text{C}}^2 \end{aligned}$$

The calculated χ^2 values fall within a range of $0 < \chi^2 < \infty$, with smaller values indicating higher spectral accuracy. In Figure 5, χ^2 values are distributed in distinct packets because at each AGC target only a restricted number of ions are stored in the C-trap. It can be seen that the SA of caffeine_{Sigma}, MRFA, and ultramark 1421 improves as the absolute ion abundance of the monoisotopic peak increases, presumably because more ions are stored in the C-trap. It should be noted that there is an upper limit to the number of charges that can be stored in the C-trap (~ 1 million charges),²⁸ and extremely high ion populations in the C-trap lead to space-charge effects, which in turn deteriorate the SA.⁴¹ Based on the previous study on SA in FT-based mass spectrometers,⁴ a χ^2 of less than 2.0 was chosen as the cutoff value for good spectral accuracy. When comparing absolute monoisotopic ion abundances corresponding to $\chi^2 < 2.0$ in caffeine_{Sigma}, MRFA, and ultramark 1421, we noticed that heavier molecules required higher absolute ion abundances for good spectral accuracy: absolute monoisotopic ion abundance of 1.9×10^4 is required to achieve high spectral accuracy in caffeine_{Sigma}, while absolute monoisotopic ion abundances of 2.0×10^4 and 4.6×10^4 are required for accurate

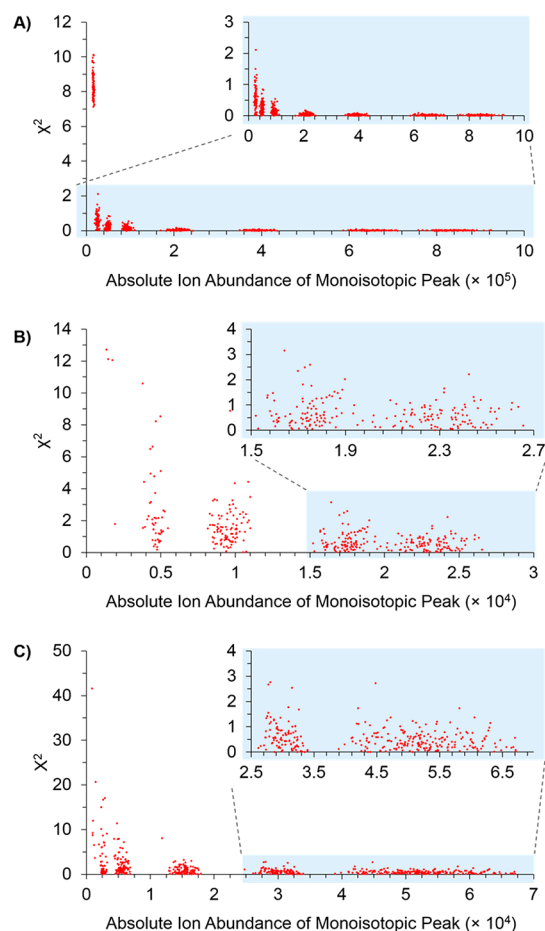


Figure 5. Pearson χ^2 distributions for (A) caffeine_{SigmaA}, (B) MRFA, and (C) ultramark 1421 across eight AGC targets. Each data point represents a single transient scan.

measurement of isotopic distributions in MRFA and ultramark 1421, respectively. These estimated absolute ion abundances can be useful in untargeted metabolomics studies, specifically in MSI, where many compounds are analyzed simultaneously.

The identification list in untargeted MSI analyses can be shortened, sometimes down to one unique elemental composition, when absolute ion abundances are above-reported thresholds. We propose a workflow for efficient elucidation of unknown elemental compositions relying on MS1 spectra only (Figure 6A). First, the user generates a list with potential IDs using m/z for monoisotopic peak (± 2.5 ppm). Next, relative abundances in the experimental isotopic distribution are used to estimate the number of atoms which in turn can help to eliminate IDs that do not match expected elemental compositions in the first list. When absolute ion abundances are above-reported minimum, estimation is highly accurate and thus chances of eliminating “correct” ID are very small. However, if absolute abundance is smaller than what we report in this work, the user may not be able to efficiently reduce the ID list because, as we have already mentioned previously, low-abundant species have a deteriorated isotopic distribution that cannot be used for accurate estimations of the number of atoms. We should also emphasize that the proposed workflow in Figure 6A will not always work. For instance, if the generated ID list has only isomers, even the highest SA will not help to distinguish those because Orbitrap-based mass spectrometers do not resolve isomeric peaks. Even though high MMA coupled

with SA does not always result in identification of unique elemental compositions, MMA and SA can definitely help to narrow down an ID list, resulting in fewer molecules to consider for MS/MS analyses.

To better explain how reported thresholds for absolute ion abundances from direct infusion experiments can be implemented in untargeted MSI analyses, we estimated the number of carbons and sulfurs in tissues with low and high absolute ion abundances of cholesterol $C_{27}H_{46}O$ (Figure 6B) and glutathione $C_{10}H_{17}N_3O_6S$ (Figure 6C,D). For carbon and sulfur counting in Figure 6, we used atom percent values (best measurements) adopted from IUPAC. Ion heat maps in Figure 6B–D were generated in MSiReader, free, open-source software for analyses of MSI files.^{42,43} The SA tools that we used for atom counting were readily implemented using MSiReader’s programming interface. These tools will be incorporated in the next free release.⁴³ When correlating carbon and sulfur counting with absolute ion abundances in healthy (low-abundant signal) and cancerous (high-abundant signal) tissues, two major points arise. First, Figures 6B–D show that carbon and sulfur counting is much more reliable in cancerous tissues with higher ion abundance than in healthy ones. This once again explains why knowing thresholds for absolute ion abundances is crucial when counting atoms. Second, Figure 6B confirms that for accurate carbon counting in a relatively small nonsulfur containing compound, at least 7.9×10^3 of $^{13}C_1$ ions are required whereas for accurate carbon (Figure 6C) and sulfur (Figure 6D) counting in a relatively small sulfur-containing compound, absolute ion abundance of $^{13}C_1$ and $^{34}S_1$ ions has to be at least 1.1×10^3 and 6.6×10^2 , respectively.

The results of the studies presented here show that while the Orbitrap is not as precise as IRMS for atomic analyses, it can be confidently used for determination of elemental compositions of unknowns at optimum ion populations. We established thresholds for absolute ion abundances that are required to achieve high SA in molecules spanning a wide mass range. The high SA in tandem with high MMA are needed to identify unknown analytes observed in untargeted IR-MALDESI MSI analyses. Current efforts are focused on implementing the screening thresholds in the image processing software MSiReader^{42,43} for automated assessment of SA of unknown analytes.

CONCLUSIONS

Elucidation of unknown elemental compositions requires not only accurately measured mass-to-charge ratios but also accurately measured relative abundances because they allow for the estimation of elemental compositions. In this work we showed that relative abundances measured in the Orbitrap ultimately depend on the number of ions injected into the mass analyzer. We also demonstrated that when absolute ion abundances are above the recommended thresholds, the Q Exactive Plus can be used for accurate estimation of the number of carbons, nitrogens, and sulfurs in small ($100 < MW$ (Da) < 400), medium ($400 < MW$ (Da) < 900), and large ($1000 < MW$ (Da) < 1500) compounds. We used caffeine_{SigmaA}, MRFA, and ultramark 1421 as representative targets for the three different mass ranges. Relative amplitudes of the resolved $^{13}C_1$ molecular isotope can predict the correct number of carbon atoms within the tolerance of less than ± 0.5 carbons when the absolute ion abundance of the $^{13}C_1$ peak is at least 7.9×10^3 in caffeine_{SigmaA}, 1.1×10^3 in MRFA, and 1.5×10^4 in ultramark 1421. Similarly,

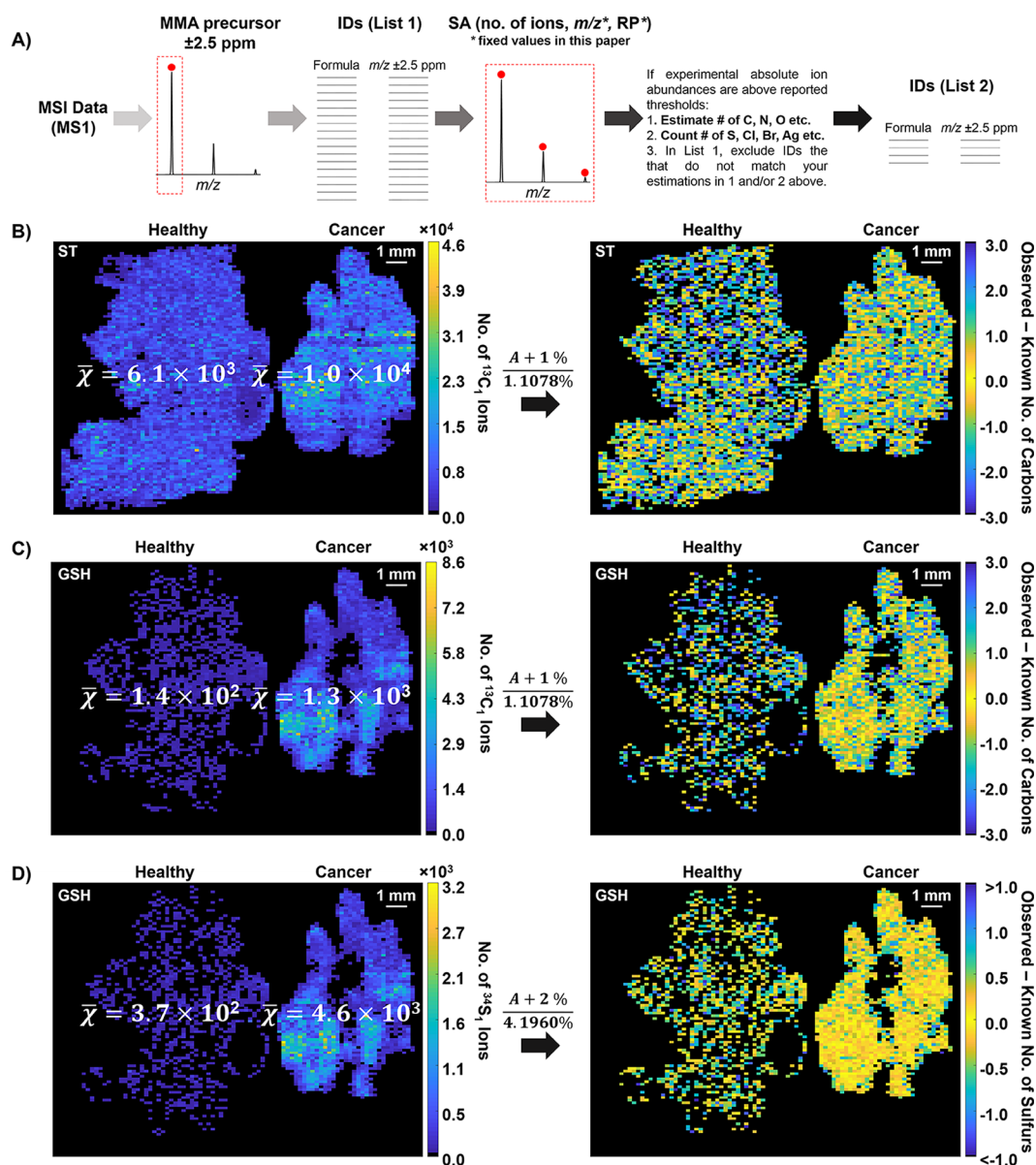


Figure 6. (A) Proposed workflow for elucidation of unknown elemental compositions in untargeted MSI experiments. (B) Ion maps for cholesterol in healthy and cancerous hen ovarian tissue sections, showing increased abundance in cancerous tissue and thus more accurate carbon counting. Ion maps for glutathione in healthy and cancerous hen ovarian tissue sections, showing increased abundance in cancerous tissue and thus more accurate (C) carbon and (D) sulfur counting. Cholesterol $[M - \text{H}_2\text{O} + \text{H}^+]^+$ and glutathione $[M - \text{H}^+]^-$ ions were generated in positive and negative ESI modes (IT = 110 ms), respectively, using 1 mM acetic acid in 50:50 MeOH:H₂O as electrospray solvent. Note that atom percent values (e.g., 1.1078%), used for carbon and sulfur counting, were adopted from IUPAC.

the abundances of the resolved isotope peaks of $^{15}\text{N}_1$ and $^{34}\text{S}_1$ enable the correct number of nitrogens and sulfurs within less than ± 0.5 atoms tolerance when absolute ion abundance of $^{15}\text{N}_1$ and $^{34}\text{S}_1$ peaks is 3.4×10^2 in caffeine_{Sigma} and 6.6×10^2 in MRFA, respectively.

Using Pearson χ^2 distributions, we have also shown that as the molecule's mass increases, more ions of that heavy molecule should be injected into the Orbitrap to accurately estimate the number of carbons, nitrogens, and sulfurs. χ^2 distributions suggest that for accurate estimation of elemental compositions in small ($100 < \text{MW (Da)} < 400$), medium ($400 < \text{MW (Da)} < 900$), and large ($1000 < \text{MW (Da)} < 1500$) compounds, absolute monoisotopic ion abundance in those compounds must be at least 1.9×10^4 , 2.0×10^4 , and 4.6×10^4 , respectively.

■ ASSOCIATED CONTENT

Supporting Information

The Supporting Information is available free of charge on the ACS Publications website at DOI: 10.1021/acs.analchem.7b03983.

Additional figures (PDF)

■ AUTHOR INFORMATION

Corresponding Author

*Phone: 919-513-0084. E-mail: david_muddiman@ncsu.edu.

ORCID

David C. Muddiman: 0000-0003-2216-499X

Author Contributions

#Authors contributed equally to this work.

Notes

The authors declare no competing financial interest.

ACKNOWLEDGMENTS

The authors gratefully acknowledge the financial support received from the National Institutes of Health (R01GM087964), the W. M. Keck Foundation, and North Carolina State University. This work was supported in part by a grant from the National Institute of Justice: NIJ 2013-DN-BX-K007. The authors also thank United States Geological Survey (Reston Stable Isotope Laboratory, Reston, VA) for measuring $\delta^{34}\text{S}$ in provided MRFA samples.

REFERENCES

- (1) Miura, D.; Tsuji, Y.; Takahashi, K.; Wariishi, H.; Saito, K. *Anal. Chem.* **2010**, *82*, 5887–5891.
- (2) Hu, Q.; Noll, R. J.; Li, H.; Makarov, A.; Hardman, M.; Graham Cooks, R. J. *Mass Spectrom.* **2005**, *40*, 430–443.
- (3) Makarov, A.; Denisov, E.; Lange, O.; Horning, S. *J. Am. Soc. Mass Spectrom.* **2006**, *17*, 977–982.
- (4) Blake, S. L.; Walker, S. H.; Muddiman, D. C.; Hinks, D.; Beck, K. *J. Am. Soc. Mass Spectrom.* **2011**, *22*, 2269–2275.
- (5) Wang, Y.; Gu, M. *Anal. Chem.* **2010**, *82*, 7055–7062.
- (6) Kind, T.; Fiehn, O. *BMC Bioinf.* **2006**, *7*, 234.
- (7) Nazari, M.; Muddiman, D. C. *Analyst* **2016**, *141*, 595–605.
- (8) Weber, R. J.; Southam, A. D.; Sommer, U.; Viant, M. R. *Anal. Chem.* **2011**, *83*, 3737–3743.
- (9) Su, X.; Lu, W.; Rabinowitz, J. D. *Anal. Chem.* **2017**, *89*, 5940–5948.
- (10) Erve, J. C. L.; Gu, M.; Wang, Y.; DeMaio, W.; Talaat, R. E. *J. Am. Soc. Mass Spectrom.* **2009**, *20*, 2058–2069.
- (11) Kind, T.; Fiehn, O. *BMC Bioinf.* **2007**, *8*, 105.
- (12) Pluskal, T. s.; Uehara, T.; Yanagida, M. *Anal. Chem.* **2012**, *84*, 4396–4403.
- (13) Erve, J. C.; Gu, M.; Wang, Y.; DeMaio, W.; Talaat, R. E. *J. Am. Soc. Mass Spectrom.* **2009**, *20*, 2058–2069.
- (14) Xu, Y.; Heilier, J.-F.; Madalinski, G.; Genin, E.; Ezan, E.; Tabet, J.-C.; Junot, C. *Anal. Chem.* **2010**, *82*, 5490–5501.
- (15) March, R. E.; Stairs, R. A.; Stock, N. L. *Int. J. Mass Spectrom.* **2017**, *415*, 18–28.
- (16) Berglund, M.; Wieser, M. E. *Pure Appl. Chem.* **2011**, *83*, 397–410.
- (17) Makarov, A. *Anal. Chem.* **2000**, *72*, 1156–1162.
- (18) Hardman, M.; Makarov, A. A. *Anal. Chem.* **2003**, *75*, 1699–1705.
- (19) Makarov, A.; Denisov, E.; Kholomeev, A.; Balschun, W.; Lange, O.; Strupat, K.; Horning, S. *Anal. Chem.* **2006**, *78*, 2113–2120.
- (20) Sampson, J. S.; Hawkridge, A. M.; Muddiman, D. C. *J. Am. Soc. Mass Spectrom.* **2006**, *17*, 1712–1716.
- (21) Bokhart, M. T.; Muddiman, D. *Analyst* **2016**, *141*, 5236–5245.
- (22) Barry, J. A.; Robichaud, G.; Bokhart, M. T.; Thompson, C.; Sykes, C.; Kashuba, A. D.; Muddiman, D. C. *J. Am. Soc. Mass Spectrom.* **2014**, *25*, 2038–2047.
- (23) Rosen, E. P.; Bokhart, M. T.; Nazari, M.; Muddiman, D. C. *Anal. Chem.* **2015**, *87*, 10483–10490.
- (24) Smith, C. A.; O'Maille, G.; Want, E. J.; Qin, C.; Trauger, S. A.; Brandon, T. R.; Custodio, D. E.; Abagyan, R.; Siuzdak, G. *Ther. Drug Monit.* **2005**, *27*, 747–751.
- (25) Wishart, D. S.; Tzur, D.; Knox, C.; Eisner, R.; Guo, A. C.; Young, N.; Cheng, D.; Jewell, K.; Arndt, D.; Sawhney, S.; et al. *Nucleic Acids Res.* **2007**, *35*, D521–D526.
- (26) Itano, W. M.; Bergquist, J. C.; Bollinger, J. J.; Wineland, D. J. *Phys. Scr.* **1995**, *1995*, 106.
- (27) Scheltema, R. A.; Hauschild, J.-P.; Lange, O.; Hornburg, D.; Denisov, E.; Damoc, E.; Kuehn, A.; Makarov, A.; Mann, M. *Mol. Cell. Proteomics* **2014**, *13*, 3698–3708.

(28) Olsen, J. V.; de Godoy, L. M. F.; Li, G.; Macek, B.; Mortensen, P.; Pesch, R.; Makarov, A.; Lange, O.; Horning, S.; Mann, M. *Mol. Cell. Proteomics* **2005**, *4*, 2010–2021.

(29) Kessner, D.; Chambers, M.; Burke, R.; Agus, D.; Mallick, P. *Bioinformatics* **2008**, *24*, 2534–2536.

(30) Bantscheff, M.; Boesche, M.; Eberhard, D.; Matthieson, T.; Sweetman, G.; Kuster, B. *Mol. Cell. Proteomics* **2008**, *7*, 1702–1713.

(31) Muccio, Z.; Jackson, G. P. *Analyst* **2009**, *134*, 213–222.

(32) Carter, J.; Fry, B. *Anal. Bioanal. Chem.* **2013**, *405*, 2799–2814.

(33) Santrock, J.; Studley, S. A.; Hayes, J. *Anal. Chem.* **1985**, *57*, 1444–1448.

(34) Brenna, J. T.; Corso, T. N.; Tobias, H. J.; Caimi, R. J. *Mass Spectrom. Rev.* **1997**, *16*, 227–258.

(35) Coplen, T. B.; Krouse, H. R. *Nature* **1998**, *392*, 32.

(36) Kozhinov, A. Fourier transform mass spectrometry at the uncertainty principle limit for improved qualitative and quantitative molecular analyses. Thesis, EPFL, Lausanne, 2015.

(37) Miladinović, S. a. M.; Kozhinov, A. N.; Gorshkov, M. V.; Tsybin, Y. O. *Anal. Chem.* **2012**, *84*, 4042–4051.

(38) Zubarev, R. A.; Makarov, A. *Anal. Chem.* **2013**, *85* (11), 5288–5296.

(39) Hu, Q.; Makarov, A. A.; Cooks, R. G.; Noll, R. J. *J. Phys. Chem. A* **2006**, *110*, 2682–2689.

(40) Gordon, E. F.; Muddiman, D. C. *J. Mass Spectrom.* **2001**, *36*, 195–203.

(41) Gorshkov, M. V.; Good, D. M.; Lyutvinskiy, Y.; Yang, H.; Zubarev, R. A. *J. Am. Soc. Mass Spectrom.* **2010**, *21*, 1846–1851.

(42) Robichaud, G.; Garrard, K. P.; Barry, J. A.; Muddiman, D. C. *J. Am. Soc. Mass Spectrom.* **2013**, *24*, 718–721.

(43) Bokhart, M. T.; Nazari, M.; Garrard, K. P.; Muddiman, D. C. *J. Am. Soc. Mass Spectrom.* **2017**, *1*–9.

NOTE ADDED AFTER ASAP PUBLICATION

This paper was published on January 11, 2018, with an error to equation 6 and Figure 6. The corrected version reposted on January 17, 2018.